General Disclaimer

One or more of the Following Statements may affect this Document

- This document has been reproduced from the best copy furnished by the organizational source. It is being released in the interest of making available as much information as possible.

- This document may contain data, which exceeds the sheet parameters. It was furnished in this condition by the organizational source and is the best copy available.

- This document may contain tone-on-tone or color graphs, charts and/or pictures, which have been reproduced in black and white.

- This document is paginated as submitted by the original source.

- Portions of this document are not fully legible due to the historical nature of some of the material. However, it is the best reproduction available from the original submission.

NASA

Technical Memorandum 78116

ON THE AVERAGE CONFIGURATION OF THE GEOMAGNETIC TAIL

D. H. FAIRFIELD

MARCH 1978

National Aeronautics and
Space Administration

Goddard Space Flight Center
Greenbelt, Maryland 20771

ON THE AVERAGE CONFIGURATION OF THE GEOMAGNETIC TAIL

D. H. Fairfield
Planetary Magnetospheres Branch
Laboratory for Extraterrestrial Physics
NASA/Goddard Space Flight Center
Greenbelt, Maryland 20771

March 1978

Submitted to the Journal of Geophysical Research

ABSTRACT

Over 3000 hours of IMP-6 magnetic field data obtained between 20 and 33 R_E in the geomagnetic tail have been used in a statistical study of the tail configuration. A distribution of 2.5 minute averages of B_z as a function of position across the tail reveals that more flux crosses the equatorial plane near the dawn and dusk flanks ($\bar{B}_z = 3.5\gamma$) than near midnight ($\bar{B}_z = 1.8\gamma$). The tail field projected in the solar magnetospheric equatorial plane deviates from the X axis due to flaring and solar wind abberation by an angle

$$\alpha = -0.9\ Y_{SM} - 1.7$$

where Y_{SM} is in earth radii and α is in degrees. After removing these effects the Y component of the tail field is found to depend on interplanetary sector structure. During an "away" sector the B_y component of the tail field is on average 0.5γ greater than that during a "toward" sector, a result that is true in both tail lobes and is independent of location across the tail. This effect means the average field reversal between northern and southern lobes of the tail is more often 178° rather than the 180° that is generally supposed.

I. INTRODUCTION

The average configuration of the geomagnetic tail has been deduced from numerous spacecraft measurements. A pair of antiparallel bundles of magnetic flux emanate from the earth's northern and southern polar caps to form two tail lobes. These lobes are separated by a diamagnetic plasma sheet of reduced field intensity (Behannon, 1970; Hruska and Hruskova, 1970; Meng and Mihalov, 1972a) which contains field lines connecting northern and southern auroral latitudes. Lobe field strengths decrease with increasing distance down the tail (Behannon, 1968; Mihalov et al., 1968). This decrease is due to (1) field lines diverging from the tail axis in both the east-west and north-south directions (Behannon, 1970; Meng and Anderson, 1974) and (2) flux lost from the lobes at larger downstream distances by crossing the equatorial plane and perhaps also the tail boundary (Mihalov et al., 1968; Behannon, 1970; Meng and Anderson, 1974). The tail axis is displaced several degrees from the earth-sun line by aberration due to the earth's motion around the sun (e.g., Behannon, 1968; Mihalov et al., 1968; Mihalov et al., 1970). Deviations of the solar wind from the radial direction will also produce variable tail orientations but these variations are generally less than 5^{o} (Wolfe, 1972) and presumably average to zero. Tail field strength is highly correlated with geomagnetic activity (eg. Behannon and Ness, 1966; Behannon, 1970; Caan et al., 1973; Meng and Anderson, 1974). Inside spacecraft apogees of 35 R_E the average field configuration exhibits a slight tendency toward a more dipolar configuration during quiet conditions (Fairfield and Ness, 1970) but this effect is not seen at 60 R_E (Meng and Anderson, 1974).

Only the average tail will be considered in the present paper: the field configuration changes associated with substorms (e.g. Fairfield and Ness, 1970) will make significant contributions to the scatter about the average values but will not be considered explicitly.

The present work extends previous statistical studies of the tail. Emphasis is placed on the east-west as well as on the north-south variations in the magnetotail structure, the former being a topic seldom considered in previous studies. Results, such as the discovery of more dipolar fields near the flanks of the tail, can be incorporated into more realistic models (e.g., Birn et al., 1977) which should lead to a better understanding of tail behavior. Dependence of the tail on interplanetary sector structure can be interpreted in terms of models linking interplanetary field lines to those of the earth.

II. DATE COVERAGE

The IMP-6 spacecraft, with a geocentric apogee of 33.1 R_E, was ideally suited to extend earlier studies of the geomagnetic tail. This spacecraft carried a tri-axial fluxgate magnetometer (Fairfield, 1974) which produced 12.5 vector measurements per second from launch on March 13, 1971 to reentry on October 2, 1974. Vector components are believed to be accurate to better than $\pm$ 0.2γ.

Intervals when this spacecraft was in the tail occurred during the months of September-November, 1971-1973. The actual intervals when the spacecraft was within the tail (this region being defined so as to include both boundary layer or plasma mantle and plasma sheet) were selected after scanning plots of both plasma data (Bame and Hones, private communication) and magnetic field data. All intervals of tail data

longer than 10 minutes were selected for analysis. A few cases where the tail could not be clearly distinguished from the magnetosheath were excluded from the data set.

The spatial coverage of IMP-6 in the tail ($X_{SM} < -20\ R_E$) is shown in Figure 1. The spacecraft trajectory is plotted in a coordinate system where Y_{SM} is the solar magnetospheric coordinate of the spacecraft (solar magnetospheric coordinates will be used throughout this paper and the subscripts will henceforth be omitted) and Z' is the estimated distance from the field reversal region or "neutral sheet":

$$\begin{aligned} Z' &= Z - (121 - .5378\ Y^2)^{1/2} \sin\chi \quad \text{for } |Y| \leq 15\ R_E \\ Z' &= Z \qquad\qquad\qquad\qquad\qquad\quad \text{for } |Y| > 15\ R_E \end{aligned} \tag{1}$$

where Y and Z are spacecraft positions and χ is the geomagnetic latitude of the sun (Fairfield and Ness, 1970).

The upper portion of the figure indicates the spacecraft location when it was within the northern lobe of the tail ($B_x > 0$) and $|\theta| \equiv |\sin^{-1} \frac{B_z}{B}| < 45^o$). The lower portion of the figure indicates the southern lobe trajectory ($B_x < 0$, $|\theta| < 45^o$). The occurrence of trajectory below (top) or above (bottom) the center line indicate times when equation 1 was unable to accurately predict the location of the midplane. Clearly equation 1 is able to predict the location of the midplane within 1 to 2 R_E the majority of the time.

To create a manageable data set, 2.5 minute averages were constructed from 15.36 second averages which were themselves averages over 192 individual vector samples. A total of 77099 such 2.5-min tail field averages

(totaling 134 days) and taken beyond X= $-20R_E$ form the basic data set used in the present paper. This quantity of data exceeds that used in the previous statistical studies (Hruška and Hrušková (1970); Fairfield and Ness (1970) and Meng and Anderson (1974).

Emphasis in this study is placed on the spatial variations in the Y and Z' directions. All data between X = -20 R_E and the 33 R_E apogee were considered equivalent and the data separated according to Y and Z' positions. This decision was made after noting that the radial variation of B from Behannon (1968) or Mihalov et al., (1968), Mihalov and Sonnett, 1968) under low K_p conditions is only from about 15 to 17γ between X = -30 and X = -20. The IMP-6 average for -25 R_E < X < -20 R_E was 17.7γ compared to 16.3γ for X < -25 R_E.

III. RESULTS

B as a function of Y and Z'. In Figure 2 the field magnitude has been plotted as a function of estimated distance from the midplane (Z' = 0) for five ranges of Y position. The data for quiet geomagnetic conditions (auroral electrojet index AE < 50γ) are shown in Figure 2a and the remainder of the data (the 87% with AE > 50γ) is shown in Figure 2b. Five curves of B vs Z' are shown for five Y sectors of the tail which are spaced symmetrically about the expected center (Y = 2 R_E) of the tail after abberration is considered. The primary difference between 2a and 2b is that the absolute magnitudes are a few gammas lower for AE < 50γ. The shapes of the curves are similar for both AE ranges with average field value near the center of the plasma sheet being about half the value of the lobe field. In the 3 central sectors of the tail the average B values associated with the plasma sheet increase

most abruptly with increasing $|Z'|$ and reach their lobe values within about $\pm$ 6 R_E of the midplane. This fact implies that the thickness of the plasma sheet near the center of the tail seldom is greater than 12 R_E and undoubtedly has an average value much less than this. On the flanks of the tail the increase of B with increasing Z' is more gradual and the average field never reaches as high a value as it does near the center of the tail. This observation seems to confirm that the plasma sheet is actually thicker near dusk and dawn as was originally determined by Bame et al. (1967), (see also Meng and Mihalov, 1972b) and that this greater thickness is not simply the result of Vela measurements being made at larger X values on the flanks (Walker and Farley, 1972). The generally lower values of B on the flanks (Fig. 2) may be due in part to the more frequent existence of the tail at large values of $|Y|$ when the magnetosheath pressure is low, the tail radius large and the field strength abnormally small.

B_Z as a function of Y and Z. Data illustrating the Y and Z' spatial variations of the B_Z component of the field are illustrated in Figure 3. In each panel of the figure, corresponding to a dawn, dusk and central portion of the tail, histograms are shown illustrating the occurrence frequency of B_Z for 2 R_E intervals of Z'. The heavy vertical tic marks through each histogram illustrate the average value of B_Z for that Z' interval. Within each Z' region, the distribution of B_Z values about the average is approximately the same, with $\sim$ 50% of the measurements falling within 1.3γ of the average value. In each Y sector the largest average values of B_Z occur near the midplane (Z' = 0) and are a measure of the average flux connecting across the midplane.

The occurrences of $B_z < 0$ at $Z' \approx 0$ may correspond to southward fields tailward of a neutral line that are being convected tailward. One must be careful, however, in interpreting the infrequent occurrence of large southward fields as lack of evidence for reconnection. If we consider a sector of the tail 1 R_E wide in Y and extending from $Z' = 0$ to $Z' = 20$, it would have a total flux ϕ_T of approximately $20\gamma \times 20\ R_E^2 = 400\gamma\ R_E^2$. If reconnection were to occur and flux were lost down the tail with a velocity V_x, the lost flux in a 1 R_E sector of Y would be $\phi = V_x B_z t$ with B_z the southward component and t the duration of the flow. With a typical velocity of 700 km/sec $\approx$ 7 R_E/min, $B_z = -2\gamma$ and $t = 2.5$ min, $\phi = 42\gamma/R_E^2$. In other words 10% of the total tail flux would be lost in 2.5 min with a southward field of 2γ. Clearly large southward fields in the presence of the large tailward flows sometimes seen in the tail can not be expected to persist for long times over wide longitudinal regions as a result of magnetic reconnection. Much detail can be lost in a 2.5 min average, a point that has been stressed recently by Coroniti et al. (1977) and Caan and Hones (1978).

In each of the panels of Figure 3 we see a gradual transition from positive B_z values near the midplane to negative values at large Z'. These negative B_z values in the tail lobes are an indication of flaring of the field away from the XY plane (Behannon, 1970; Meng and Anderson, 1975). A representative value of $B_z = -2\gamma$ at $Z' = 14\ R_E$ is associated with a field strength of 20γ and therefore corresponds to a flaring angle of 5.7°. This gradual transition from positive B_z to negative B_z with increasing Z' was not apparent in the IMP 4 data of Fairfield and Ness (1970). This difference apparently was due to the fact that during the

single three-month traversal of IMP 4 through the tail, this spacecraft preferentially sampled the southern lobe near dawn, the northern lobe near dusk and the midplane near the center of the tail. Note in Figure 3 that B_z values several R_E away from the midplane near dawn and dusk are approximately 2γ as is B_z at $Z' \approx 0$ in the center of the tail. Apparently non-uniform sampling along with a variation of B_z with Y conspired to give B_z an approximately constant average value in the IMP 4 data.

To pursue this Y dependence of B_z, the tail was divided into five sectors spaced symmetrically about the $Y = 2\ R_E$ plane in the tail. These average values of B_z as a function of Z' are shown in Figure 4 for AE ranges below (4a) and above (4b) 50γ. Clearly B_z is largest near the dawn boundary, slightly smaller near the dusk boundary, and is still smaller and relatively uniform across the central portion of the tail. This effect may be enhanced during quiet times, although the smaller amount of data for $AE < 50$ makes this conclusion less certain. These results are consistent with those of Meng and Anderson (1974) although, since they investigated distributions of the absolute values of θ and B_z, their work does not make clear that the fields were more northward near dusk and dawn. The large values of B_z near dusk and dawn are consistent with a thick plasma sheet in these regions and also suggest that any tail neutral line may be nearer the earth near Y = 0 and curve tailward near the flanks (Russell, 1977).

Negative B_z is rarely seen near the flanks of the tail, a result that is in conflict with reports by Frank et al., (1976) of a persistent zone of southward field in the boundary layer near the flanks. This discrepancy undoubtedly is due to differing judgements in the two studies as to which data intervals are within the magnetosphere boundary layer and which are in the magnetosheath.

B_y in the Tail

The distribution of Y values in the tail is influenced primarily by the facts that (1) the tail is skewed away from the X axis by the aberration angle caused by the earth's motion around the sun and (2) the tail flares away from the center line of the tail (the aberrated X axis). These effects can be seen in Figure 5 which is in the format of Figure 3 except data are for the B_y component. Flaring of the fields away from the center of the tail produce positive B_y values in the northern dawn and southern dusk quadrants and negative values in the southern dawn and northern dusk sectors. The aberration of the entire tail adds to the flaring angle in the dusk hemisphere and substracts from it near dawn, causing the magnitude of the B_y component to be larger at dusk than at dawn. The spread of B_y values about the averages is comparable to that seen in B_z.

In order to eliminate skewing and aberration effects and be able to study additional variations in B_y, it was necessary to calculate the average angle between the solar magnetospheric equatorial component of the tail field and the X axis. To do this, the data were divided among 5 ranges of Y in the region $X < -20$. In each range the average solar magnetospheric B_x and B_y components were calculated separately for the northern and southern hemisphere. Data taken in the equatorial region $|Z'| < 3\ R_E$, where the field might sometimes be primarily in the Z direction, were eliminated as were occasional odd points where an earthward (tailward) pointing tail field was observed in the southern (northern) hemisphere. The flaring angle of the field in the equatorial plane, $\alpha = \tan^{-1} \bar{B}_y/\bar{B}_x$, was calculated for the northern and southern hemispheres independently.

These angles are shown by the open and closed circles respectively in Figure 6 where they are plotted at the average position within the sector. The weighted average of the northern and southern hemisphere points in each region was calculated and is represented by the crosses in Figure 6. A linear least squares fit to these five crosses give the line in Figure 6 which is represented by the equation

$$\alpha = -0.9\ Y - 1.7 \qquad (1)$$

where Y is in earth radii and α is in degrees.

Note that if the aberration of the tail is 4°, we may set α equal to -4° in equation 1 and find that the effective center of the tail in the range $-33 < X < -25\ R_E$ is at $Y_{SM} = 2.6\ R_E$. In other words, the axis of the tail $\sim 30\ R_E$ behind the earth passes through a point displaced $2.6\ R_E$ from the X axis, a number roughly consistent with the original division of the tail where $2\ R_E$ was assumed. The value of $0.9^{\circ}/R_E$ for the rate of increase of the flaring angle is 50% greater than that found by Mihalov et al. (1970) at $60\ R_E$. This is not surprising and suggests that the flaring decreases at larger distances down the tail.

Meng and Anderson (1974) also found somewhat different results at $60\ R_E$. In their study, the $|B_y|$ component did not increase appreciably near the dawn boundary of the tail where the average angle the field made with the X axis did not exceed 2°. Near the dusk boundary of the tail Meng and Anderson found a flaring angle of -12° (the negative direction being that of increasing aberration in accord with the convection of Figure 6). These angles may be contrasted with corresponding angles of 16.3 and -23.3° calculated from equation 1 at average tail boundaries of $Y_{SM} = -20\ R_E$ and $Y_{SM} = 24\ R_E$ and again suggest a decrease in flaring at larger distances.

The ability of equation 1 to predict the flaring and aberration of the tail is illustrated in Figure 7. The format is that of Figures 3 and 5 but now each 2.5-minute average measurement is rotated by the angle α predicted by equation 1 before inclusion in the histogram. Clearly the average flaring and aberration effects are well removed. Scatter about the averages is reduced so that the standard deviation is 1.7γ. The negative B_y averages in the dusk sector indicate that the rotation was not enough in the northern hemisphere and too much in the southern hemisphere, a result that is both consistent with the northern and southern hemisphere points below and above the average in Figure 6 and also with the surprising findings of Meng and Anderson (1974) that northern hemisphere fields flare away from the Y = 0 plane more than those of the south.

It is of interest to look for the effects of field aligned currents in Figure 7. Small scale field aligned currents are known to flow on the boundary of an expanding plasma sheet during substorms (Aubry et al. 1972; Fairfield, 1973) and it might be expected that the more persistent and larger-scale currents seen at low altitudes in the night hemisphere (Iijima & Potemra, 1976; Sugiura and Potemra, 1976) would be detectable in the same plasma-sheet boundary region. The higher latitude or "region 1" currents of Iijima and Potemra are those which would extend into the tail (Potemra, 1977). These currents flow toward the ionosphere in the dawn hemisphere and away from the earth in the dusk hemisphere. If we approximate a region 1 current by a sheet current which extends into the tail and is aligned with the plasma sheet boundary, then a spacecraft in the dawn hemisphere would expect to detect a negative (positive) B_y perturbation in the northern (southern) tail lobes and the reverse perturbation in the plasma

sheet on the opposite side of the sheet. In the dusk hemisphere all signs would reverse as the current direction reverses. To estimate the expected magnitude of these perturbations in the tail, we assume that a sheet of 30^{o} longitudinal extent maps to a sector 8 R_E wide in the tail ($\sim$ 1/5 the east-west dimension of the tail). The 30^{o} longitudinal width at 68^{o} latitude and 800 km altitude (the altitude of the Triad spacecraft of Iijima and Potemra) corresponds to a dimension of 1400 km. When this sheet expands to 8 R_E in longitudinal width, the current intensity/km longitude is reduced by a factor of 36. Typical low latitude magnetic perturbations of 200-400γ (Sugiuia and Potemra, 1976) should be reduced by the same factor, leading to an estimate of 5.5-11γ for the perturbations in the tail. Certainly no such effects are seen in Figure 7. In fact, little evidence is seen for any such currents in Figure 7 except, perhaps, for the negative values in the northern-most dawn region.

In considering why the effects of field aligned currents in the tail are not observed, we must first realize that the current sheet model is an over simplification of the actual situation. The low altitude currents have typical latitudinal widths of several degrees and will project to a rather extended region of the tail. The location of the tail currents undoubtedly change as the plasma sheet expands and contracts, an effect that will lead to positive and negative perturbations cancelling each other in a long term average. Also the spacecraft distance to the primary current region is not always small compared to the distance to other currents in the tail such as the lower-latitude "region 2" currents and the oppositely directed currents of the dawn or dusk hemisphere further from the spacecraft.

Another effect will tend to obscure B_y perturbations in the tail lobes. The largest field-aligned currents flow during geomagnetically disturbed times (Iijima and Potemra, 1976) when the tail field tends to be large. This larger tail field is due to an increased amount of flux in the tail (e.g., Maezawa, 1975) and a resulting larger flaring angle. This increased flaring angle along with an increased field strength will produce an increased B_y perturbation in the tail lobes which is of the opposite sign to that produced by the field aligned currents that are expected to flow. These two effects will always tend to cancel in the tail lobes. In the plasma sheet the two effects will add but the field strength is smaller in this region. This reasoning suggests that the plasma sheet fields diverge more rapidly from the tail axis than the lobe fields. The fact that the B_y components in Figure 7 are constant as a function of Z', even though they have been rotated through the same angles as the lobe fields, is consistent with this idea.

Whether the lack of evidence for field aligned currents in the tail can be explained by the above considerations is not clear. The more quantitative models necessary to answer this question are beyond the scope of the paper.

B_y Dependence on Interplanetary Sector Structure

In view of the many high-latitude phenomena that depend on the polarity of the interplanetary magnetic field, the dependence of B_y on this parameter was investigated. All tail intervals were separated according to whether they occurred during "toward" or "away" interplanetary sectors (Fairfield and Ness, 1974 and references therein). The B_y averages with flaring-aberration effects removed are shown in Figure 8

for various Z' values and for three Y intervals. For almost every Z' interval and Y sector the toward sector curves have smaller B_y components, the average difference for the three sectors being 0.5, 0.4 and 0.7γ going from dawn to dusk. Although standard deviations in the three sectors are 1.70, 1.65, and 1.60γ, the large number of observations lead to a standard error of the mean of the order of 0.02γ for the separate tail regions in each of the interplanetary sectors. A statistical t test indicates that the toward-away differences are significant at better than the 99% confidence level. A geometrical description of this result is given in the Figure 8 insert. During a toward sector a small negative B_y component added to both of the anti-parallel fields of the two tail lobes means that the fields are no longer oriented 180^o apart. If 0.25γ are added to 15γ X-axis-aligned fields, the antiparallel fields then make an angle of 178^o. The effect is in the opposite direction for fields of the other polarity.

To further pursue this result, a direct comparison was made between tail B_y components and the simultaneously measured interplanetary field. The flaring-aberration effects were again removed using equation 1 and hourly averages were constructed for comparison with solar magneto-spheric B_y hourly averages (King, 1977). A scatter plot of B_y(Tail) vs. B_y(IP) is shown in Figure 9. Although a great deal of scatter is present, averaging B_y(Tail) over 1γ intervals of B_y(IP) reveals the expected trend. A least-squares fit to these averages points yields the equation $B_y(\text{Tail}) = .13\ B_y(\text{IP}) - 0.30$. If we take $B_{y\text{IP}} = 2\gamma$ and -2γ as values for the average interplanetary B_y component, we can reproduce the 0.5γ average difference for tail fields in the two interplanetary sectors. A visual scanning of

simultaneous tail and interplanetary magnetic field plots suggests that sudden changes in the B_yIP are not obviously reflected in sudden changes in B_yTail. This observation suggests that the B_yTail may respond to the interplanetary field more on a scale of hours or days than minutes.

This sector dependence of B_y may be relevant in explaining a surprising result of Meng and Anderson (1974). These authors analyzed Explorer 35 data at the lunar orbit and found that the magnetic field in the southern lobe of the tail averaged over all longitudes is aligned closer to the X axis than is the northern lobe. This configuration is identical to that found above when the tail is in a toward sector and hence it is of interest to ask whether the Explorer 35 data used by Meng and Anderson was taken preferentially in toward sectors. Using the intervals of the 34 tail passes of Explorer 35 in 1967-1970 (Meng and Milhalov, 1972a) and interplanetary sector information (Fairfield and Ness, 1974; and references therein) it is found that indeed 20% more data was taken in toward sectors than away sectors. This imbalance is consistent with an unusual predominance of negative polarity during these years (Fairfield and Ness, 1974, Figure 5). The sector structure effect is in the right sense to explain the north-south dependence of Meng and Anderson although the magnitude of the latter effect (approximately a 6^{o} difference between average north and south directions) seems too large to be fully accounted for unless the sector dependence is larger at 60 R_E than near 30 R_E.

IV. SUMMARY AND CONCLUSIONS

A statistical study of the geomagnetic tail has recorded large-scale variations in the field configuration in both the north-south

and east-west directions. The largest values of B_z occur near the midplane of the tail. At greater distances from the midplane, B_z decreases as field lines become more horizontal. Above $|Z'| \approx 9\ R_E$, B_z is negative as open field lines diverge from the equatorial plane. Average B_z values near dusk and especially dawn are about a factor of two greater than those near $y = 0$ implying more dipolar field lines near the flanks of the tail. The diamagnetic depression in the field strength has a broader spatial extent near the flanks suggesting that a thicker plasma sheet exists in this region. This result is consistent with the more dipolar field lines near the flanks which are better able to confine the plasma of a thick plasma sheet. This larger B_z near the flanks suggests that on the average a neutral line across the tail where $B_z = 0$ must curve away from the earth so that it is further down the tail on the flanks (Russell, 1977). The divergence of the field lines from the midnight meridian plane is found to be given by an angle $\alpha = -0.9Y - 1.7$. This tail flaring near the boundaries is about twice that seen at 60 R_E which suggests that the flaring angle decreases with increasing distance down the tail. The effects of low-altitude large-scale field-aligned currents extending to the tail are not observed.

The standard deviation associated with the average field components in the tail is of the order of 2γ. These variations are thought to be due to the following effects: (1) Changes in solar wind speed and direction will move the axis of the tail (a 3^o rotation of a 20γ field directed along the X axis will produce a 1.0γ transverse field component); (2) Changes in the field during substorms will vary the flaring angle in the tail (increased tail flux will produce larger flaring angles which imply

larger magnetosheath pressures and larger field strengths. Both the large strengths and larger flaring angles will lead to larger B_z and B_y components; (3) Changes in solar wind pressure will vary the flaring angle of the tail field and its magnitude; (4) Waves in the tail magnetic field will produce B_y and B_z components and contribute to scatter about the averages.

An additional result of this study is that the average B_y component of the tail field is about 0.5γ larger during an away interplanetary sector than in a toward sector, a result that is true in northern and southern hemispheres and in all longitudinal sectors of the tail. This B_y sector dependence has a possible interpretation in terms of the magnetosphere reconnection model. Stern (1973) has emphasized how reconnected field lines must leave the magnetosphere through a relatively small region or "window" whose location depends on the direction of the interplanetary field. Current thinking (e.g., Fairfield, 1977 and references therein) suggests that in an away sector (interplanetary $B_y > 0$) dayside reconnection occurs at high latitudes in the northern dusk and southern dawn regions. The portions of the reconnected field lines that lead directly to the earth have their interplanetary ends on the dawn and dusk sides of the earth in the northern and southern hemispheres respectively. As they convect toward the tail their exit region or window is on the dawn or dusk side in the north and south respectively. Skewing of the entire tail lobe in the direction of the exit window can explain the observed results. All signs and directions reverse in a sector with the opposite polarity.

A final result is a lack of negative B_z near the dawn and dusk boundaries: a result that is in conflict with that of Frank et al. (1976)

who find a persistent zone of southward field in the boundary layers of this region. This discrepancy must be resolved by a careful study that uses detailed measurements to make unambiguous separations of the boundary layer from the magnetosheath.

ACKNOWLEDGMENTS

The author gratefully acknowledges useful discussions with Dr. T. A. Potemra of the Applied Physics Lab, Dr. D. P. Stern and numerous other colleagues at Goddard Space Flight Center. The programming support of Mr. Praedeep Simlote is also much appreciated. Plasma data used in defining tail intervals was provided by E. W. Hones, Jr. and S. J. Bame of the Los Alamos Scientific Laboratory.

FIGURE CAPTIONS

Figure 1. Trajectory of IMP 6 in the geomagnetic tail in a coordinate system where Z' is the estimated distance from the midplane and Y_{SM} is the solar magnetospheric Y position. Earthward-polarity-field intervals are shown on the upper axes and tailward-pointing-field intervals on the lower axes. Data are for $X_{SM} < -20\ R_E$.

Figure 2. Average field strength as a function of distance from the tail midplane for AE < 50 and AE > 50. The five curves in each panel correspond to five east-west sectors of the tail.

Figure 3. Histograms of B_z for 2 R_E intervals of Z' in dawn, dusk and central portions of the tail beyond 20 R_E. The vertical bars through each histogram indicate the average B_z for that Z' interval.

Figure 4. Average B_z as a function of Z' for AE < 50γ and AE > 50γ. Five curves in each panel correspond to five east-west sectors of the tail.

Figure 5. Histograms of the B_y component of the tail field in the same format as Figure 3.

Figure 6. The average angle between the tail field projected into the solar magnetospheric equatorial plane and the X axis is plotted as a function of position across the tail.

Figure 7. B_y histograms equivalent to Figure 5 except that the average flaring-aberration effects have been removed from individual data samples using the equation of Figure 6.

Figure 8. Average B_y values at various distances from the midplane in three Y position sectors. Data are separated according to whether the tail was immersed within a toward or away interplanetary sector. B_y in away sectors is greater than that in toward sectors for almost every interval of Z' and Y.

Figure 9. Hourly averages of interplanetary B_y are plotted vs. the simultaneously measured hourly averages of B_y in the tail with average configuration effects removed. Circles indicate average tail B_y for 1γ intervals of interplanetary B_y.

REFERENCES

Aubry, M.P., M.G. Kivelson, R.L. McPherron, C.T. Russell, and D.S. Colburn, "Outer Magnetosphere Near Midnight at Quiet and Disturbed Times", J. Geophys. Res., 77, 5487, 1972.

Bame, S.J., J.R. Asbridge, H.E. Felthauser, E.W. Hones, and J.B. Strong, "Characteristics of the Plasma Sheet in the Earths Magnetotail", J. Geophys. Res., 72, 113, 1967.

Behannon, K. W., "Mapping of the Earth's Bow Shock and Magnetic Tail by Explorer 33", J. Geophys. Res., 73, 907, 1968.

Behannon, K.W., "Geometry of the Geomagnetic Tail", J. Geophys. Res., 75, 743, 1970.

Behannon, K.W. and N.F. Ness, "Magnetic Storms in the Earth's Magnetic Tail", J. Geophys. Res., 71, 2327, 1966.

Birn, J., R.R. Sommer, and K. Schindler, "Self Consistent Theory of the Quiet Magnetotail in Three Dimensions", J. Geophys. Res., 82, 147, 1977.

Caan, M.N., R.L. McPherron, and C.J. Russell, "Solar Wind and Substorm-Related Changes in the Lobes of the Geomagnetic Tail", J. Geophys. Res., 78, 8087, 1973.

Caan, M. N. and E.W. Hones, Jr., Comment on "Search for the Magnetic Neutral Lines in the Near-Earth Plasma Sheet, 2. Systematic Study of IMP-6 Magnetic Field Observations", by A.T. Y. Lui, C.-I. Meng and S.-I. Akasofu, submitted to J. Geophys. Res., 1977.

Coroniti, F.V., F.L. Scarf, L.A. Frank and R.P. Lepping, "Microstructure of a Magnetotail Fireball", Geophys. Res. Lett., 4, 219, 1977.

Fairfield, D.H., "Magnetic Field Signatures of Substorms on High-Latitude Field Lines in the Nighttime Magnetosphere, J. Geophys. Res., 78, 1553, 1973.

Fairfield, D.H., "Whistler Waves Observed Upstream from Collisionl-Shocks", J. Geophys. Res., 79, 1368, 1974.

Fairfield, D.H., "Electric and Magnetic Fields in the High-Latitutde Magnetosphere", Rev. Geophys. Space Phys., 15, 285, 1977.

Fairfield, D.H. and N.F. Ness, "Configuration of the Geomagnetic Tail During Substorms", J. Geophys. Res., 75, 7032, 1970.

Fairfield, D.H. and N.F. Ness, "Interplanetary Sector Structure: 1970-1972", J. Geophys. Res., 79, 5089, 1974.

Frank, L.A., K.L. Ackerson and R. P. Lepping, "On Hot Tenuous Plasmas, Fireballs, and Boundary Layers in the Earth's Magnetotail", J. Geophys. Res., 81, 5859, 1976.

Hruška, A. and J. Hrušková, "Transverse Structure of the Earth's Magnetotail and Fluctuations of the Tail Magnetic Field", J. Geophys. Res., 75, 2449, 1970.

Iijima, Takesi and T.A. Potemra, "The Amplitude Distribution of Field-Aligned Currents at Northern High Latitudes Observed by Triad", J. Geophys. Res., 81, 2165, 1976.

King, J. H., "Interplanetary Medium Data Book, Natural Space Science Data Center publication No. 77-04, Greenbelt, MD, 1977.

Maezawa, Kiyoshi, "Magnetotail Boundary Motion Associated with Geomagnetic Substorms", J. Geophys. Res., 80, 3543, 1975.

Meng, C.-I and J.D. Mihalov, "On the Diamagnetic Effect of the Plasma Sheet Neart 60 R_E", J. Geophys. Res., 77, 4661, 1972.

Meng, C.-I and J.D. Mihalov, "Average Plasma-Sheet Configuration near 60 Earth Radii", J. Geophys. Res., 77, 1739, 1972.

Meng, C.-I. and K.A. Anderson, "Magnetic Field Configuration in the Magnetotail near 60 R_E", J. Geophys. Res., 79, 5143, 1974.

Mihalov, J.D. and C.P. Sonett, "The Cislunar Geomagnetic Tail Gradient in 1967", J. Geophys. Res., 73, 6837, 1968.

Mihalov, J.D., D.S. Colburn, R.G. Currie and C.P. Sonett, "Configuration and Reconnection of the Geomagnetic Tail", J. Geophys. Res., 73, 943, 1968.

Mihalov, J.D., D.S. Colburn and C.P. Sonett, "Observations of Magnetopause Geometry and Waves at the Lunar Distance", Planet. Space Sci., 18, 239, 1970.

Potemra, T.A., "Large-Scale Characteristics of Field-Aligned Currents Determined from the Triad Magnetometer Experiment, in Dynamical and Chemical Coupling Between Neutral and Ionized Atmosphere", B. Grandel and J.A. Holtet, eds. D. Reidel, Dordrecht Holland, 337, 1977.

Russell, C.T., "Some Comments on the Topology of the Geomagnetic Tail", J. Geophys. Res., 82, 1625, 1977.

Stern, David P., "A Study of the Electric Field in an Open Magnetospheric Model", J. Geophys. Res., 78, 7292, 1973.

Sugiura, Masahisa and Thomas A. Potemra, "Net Field-Aligned Currents Observed by Triad", J. Geophys. Res., 81, 2155, 1976.

Walker, R.J. and T.A. Farley, "Spatial Distribution of Energetic Plasma Sheet Electrons", J. Geophys. Res., 77, 4650, 1972.

Wolfe, John H., "The Large-Scale Structure of the Solar Wind, in Solar Wind, edited by C.P. Sonett et al., NASA SP-308, 170, 1972.

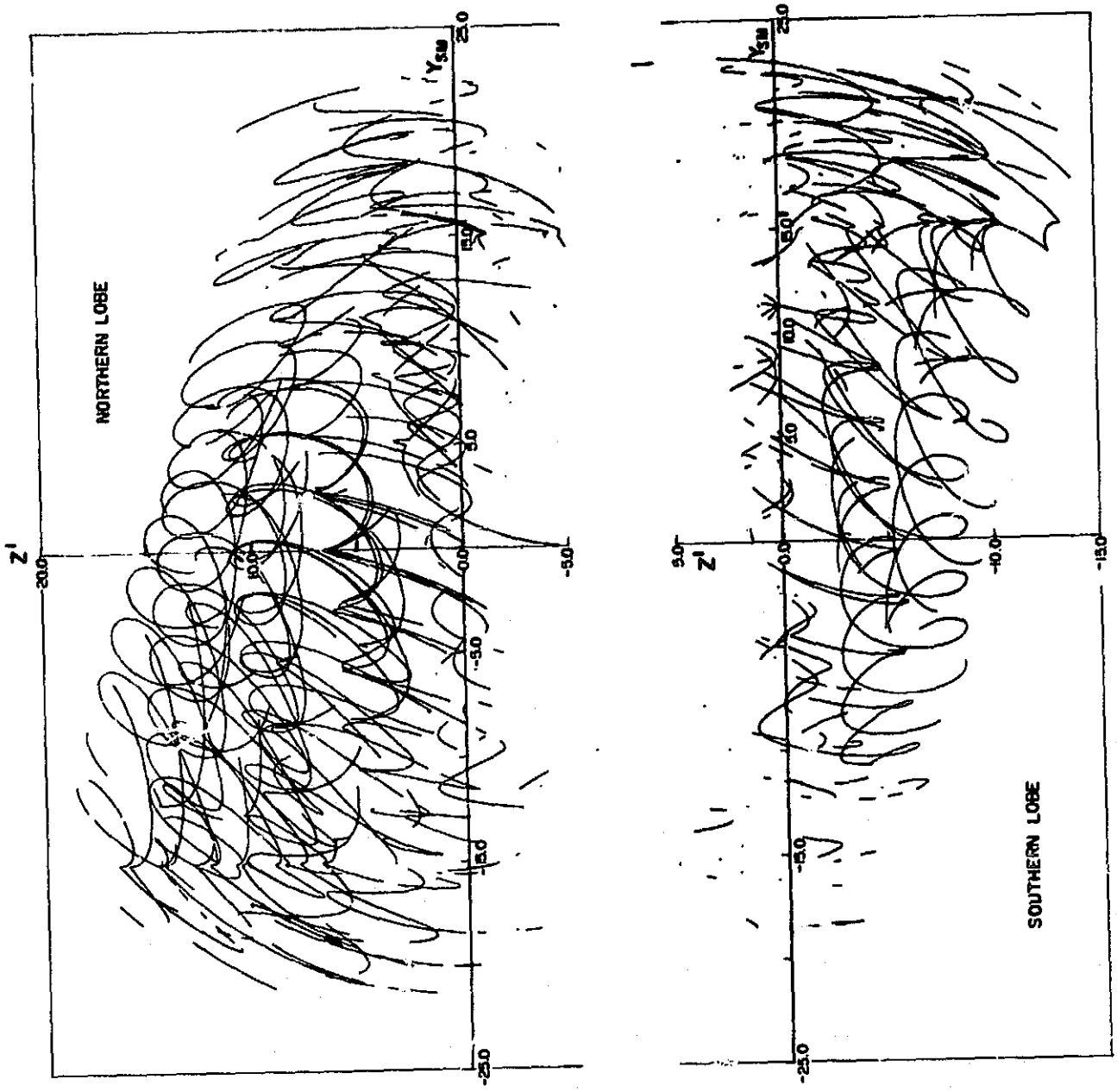

Figure 1

ORIGINAL PAGE IS
OF POOR QUALITY

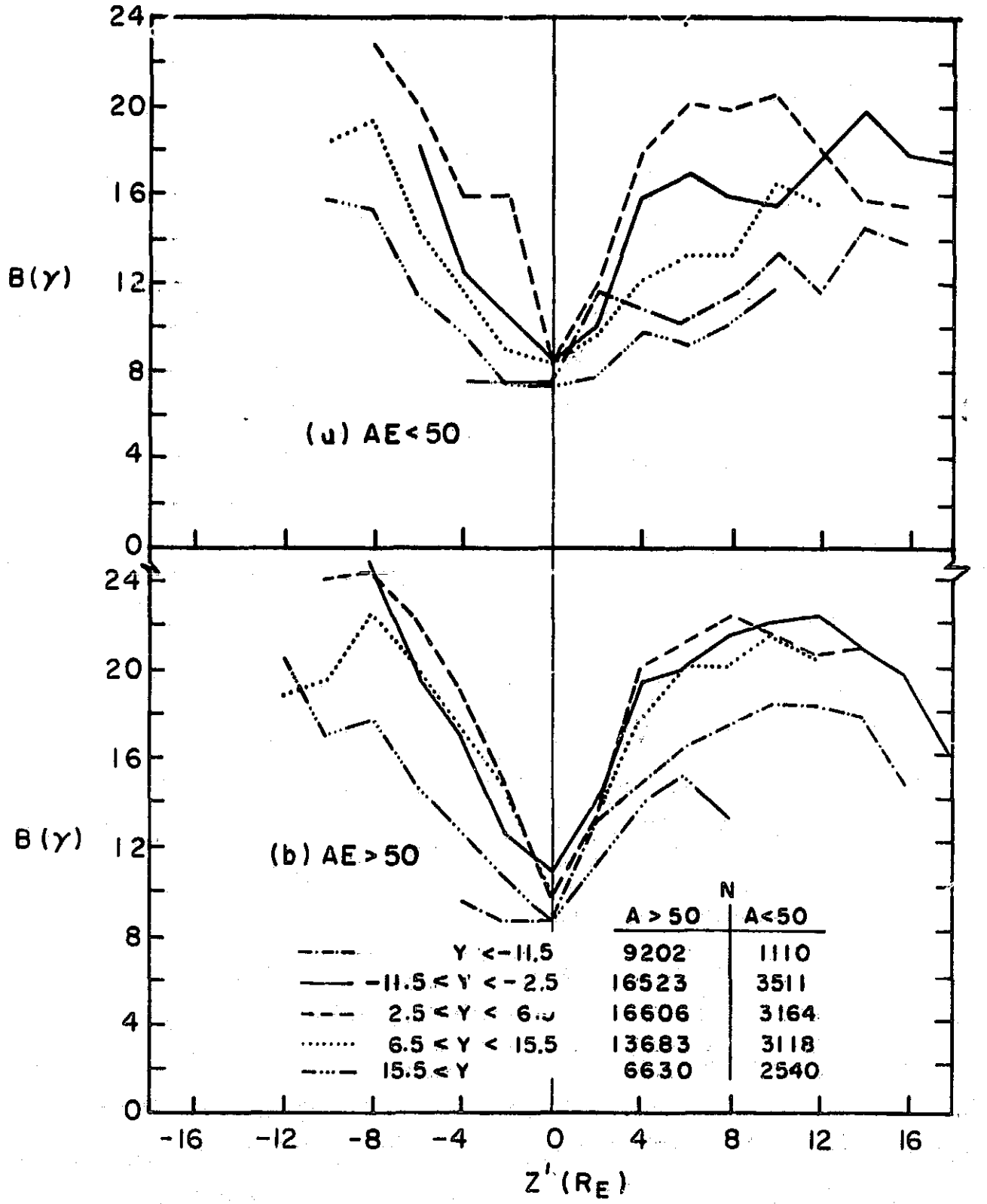
B(γ)
(a) AE<50
(b) AE>50
B(γ)
N
A>50 A<50
Y <-11.5 9202 1110
-11.5<Y<-2.5 16523 3511
2.5<Y< 6.5 16606 3164
6.5<Y<15.5 13683 3118
15.5<Y 6630 2540
Z' (R_E)

Figure 2

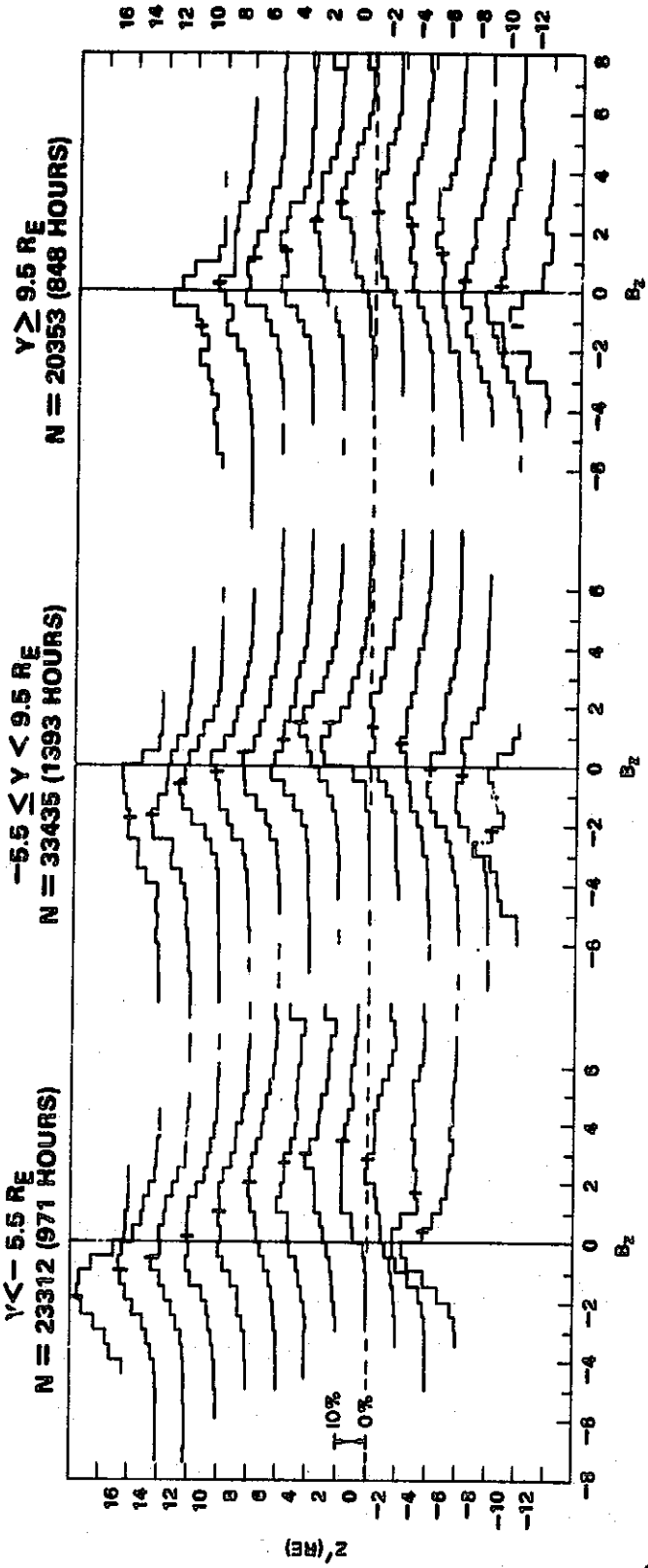

Figure 3

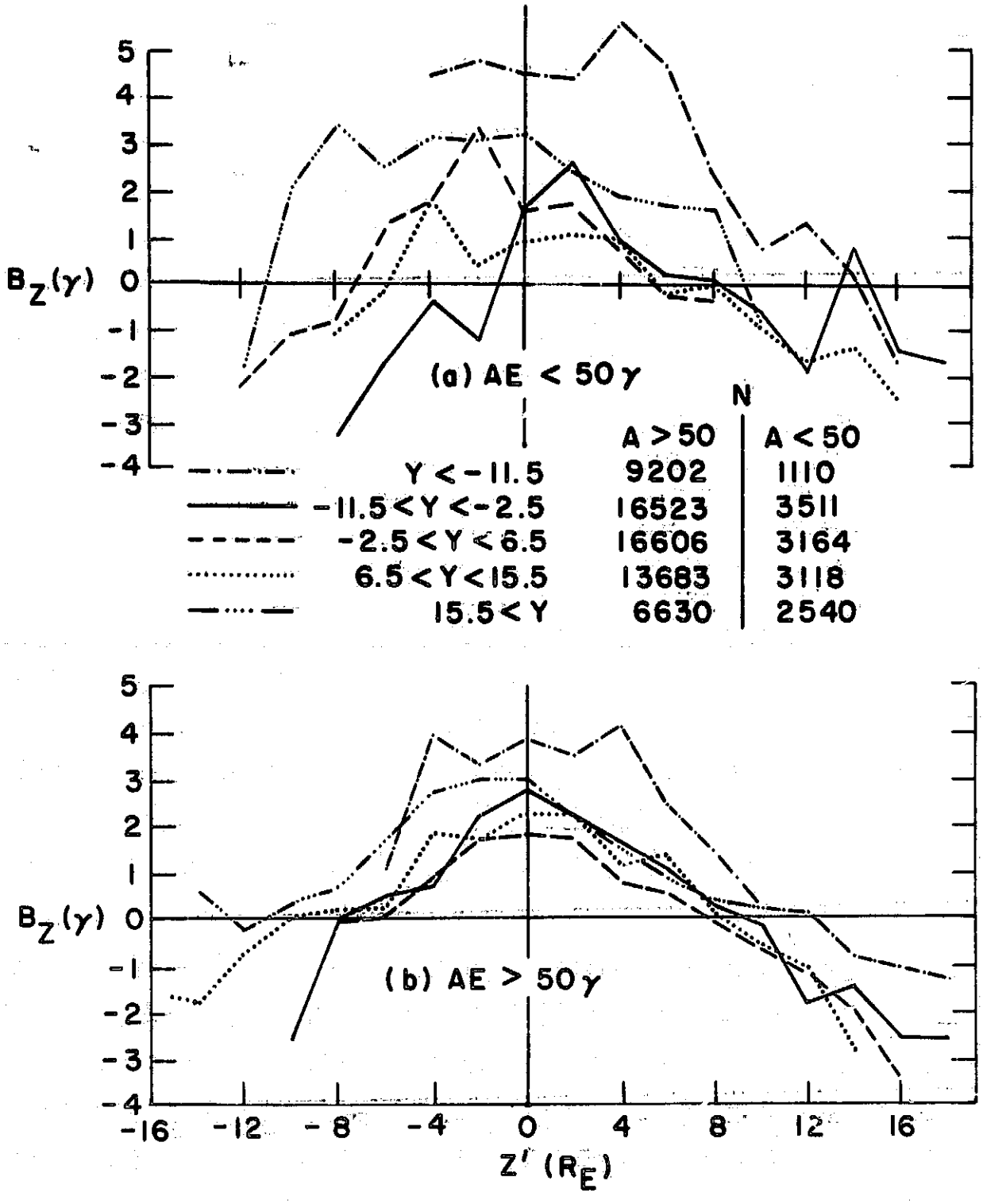
5
4
3
2
1
0
-1
-2
-3
-4
$B_Z(\gamma)$
(a) AE < 50γ
N
A > 50
A < 50
Y < -11.5
9202
1110
-11.5 < Y < -2.5
16523
3511
-2.5 < Y < 6.5
16606
3164
6.5 < Y < 15.5
13683
3118
15.5 < Y
6630
2540
(b) AE > 50γ
-16
-12
-8
-4
0
4
8
12
16
Z' (R_E)

Figure 4

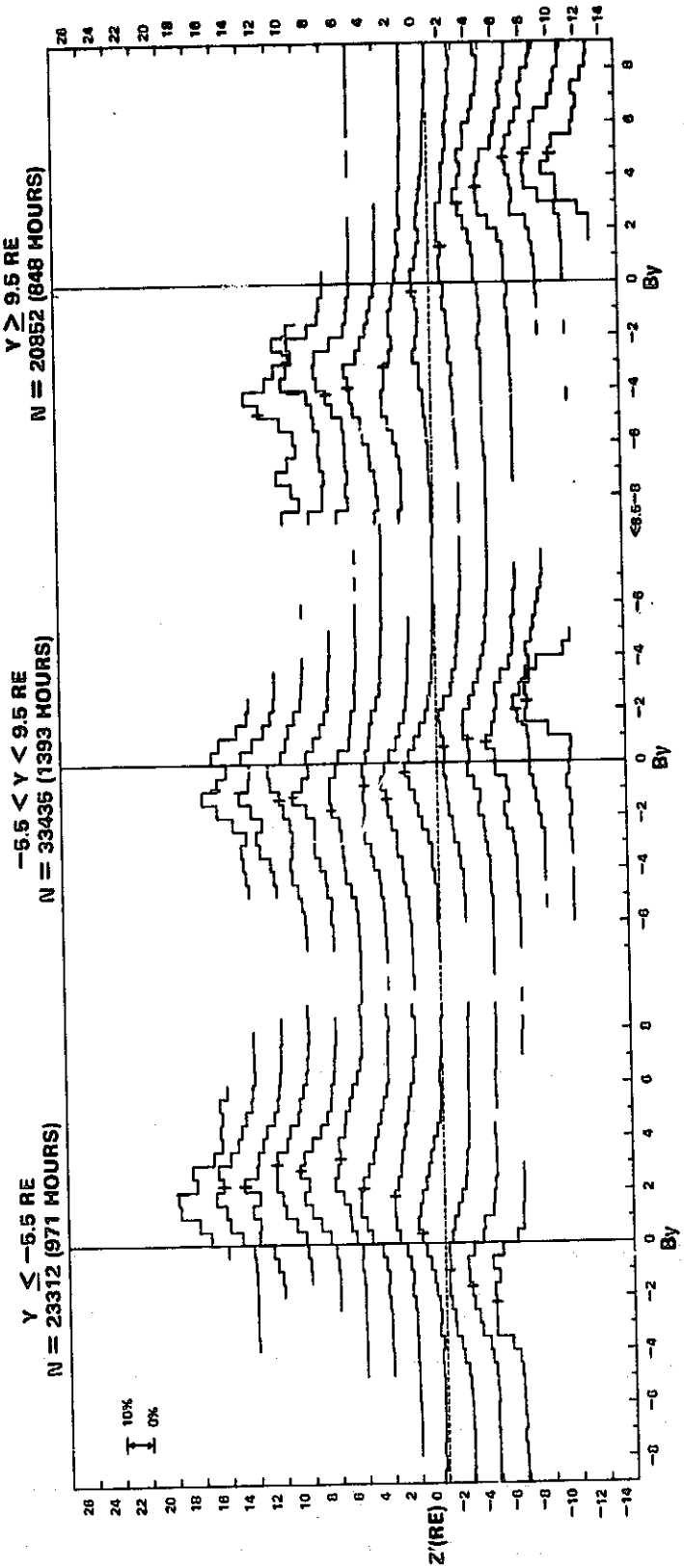

Figure 5

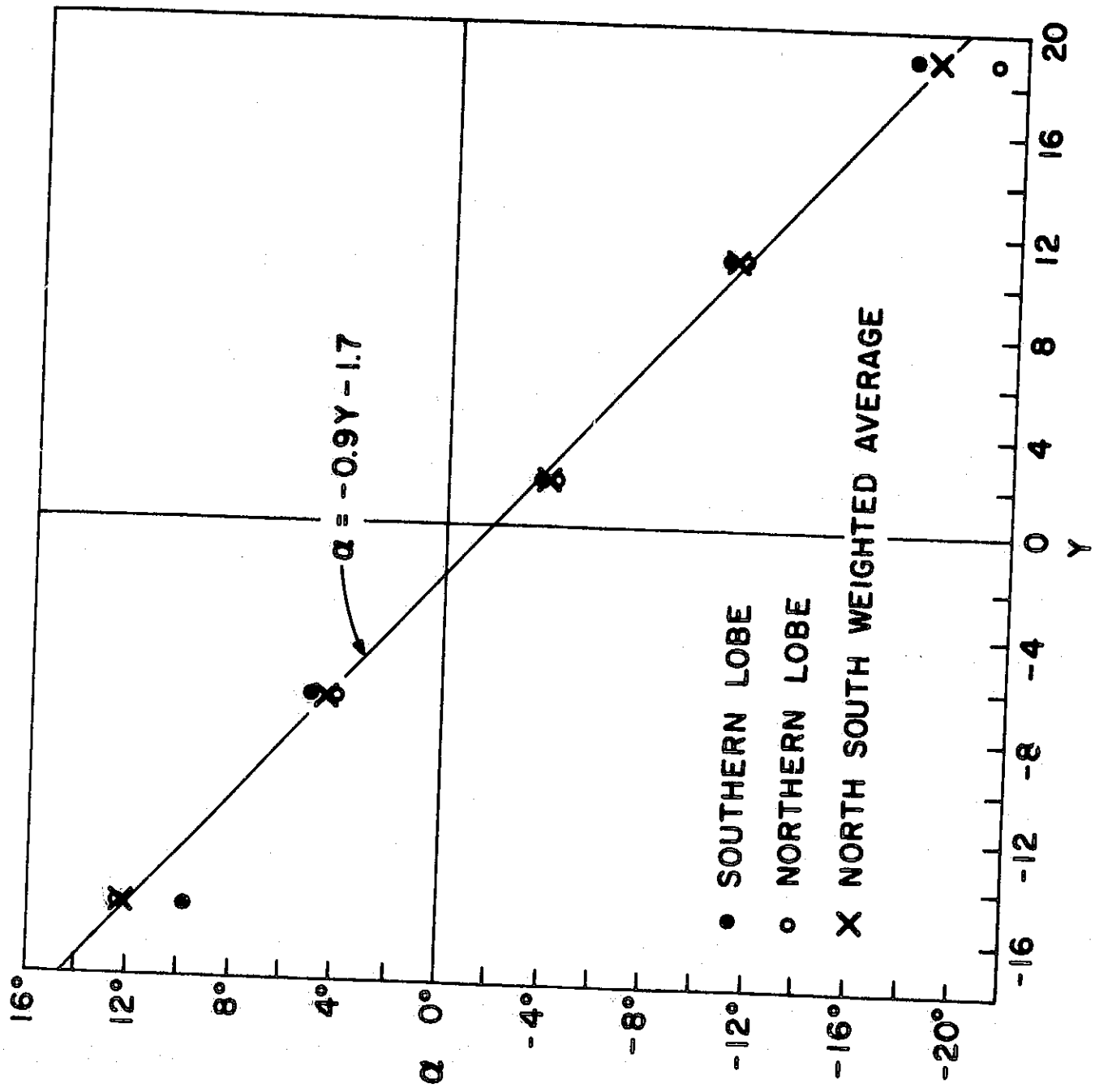
α = -0.9Y - 1.7
• SOUTHERN LOBE
o NORTHERN LOBE
X NORTH SOUTH WEIGHTED AVERAGE
α
Y
16°
12°
8°
4°
0°
-4°
-8°
-12°
-16°
-20°
-16
-12
-8
-4
0
4
8
12
16
20

Figure 6

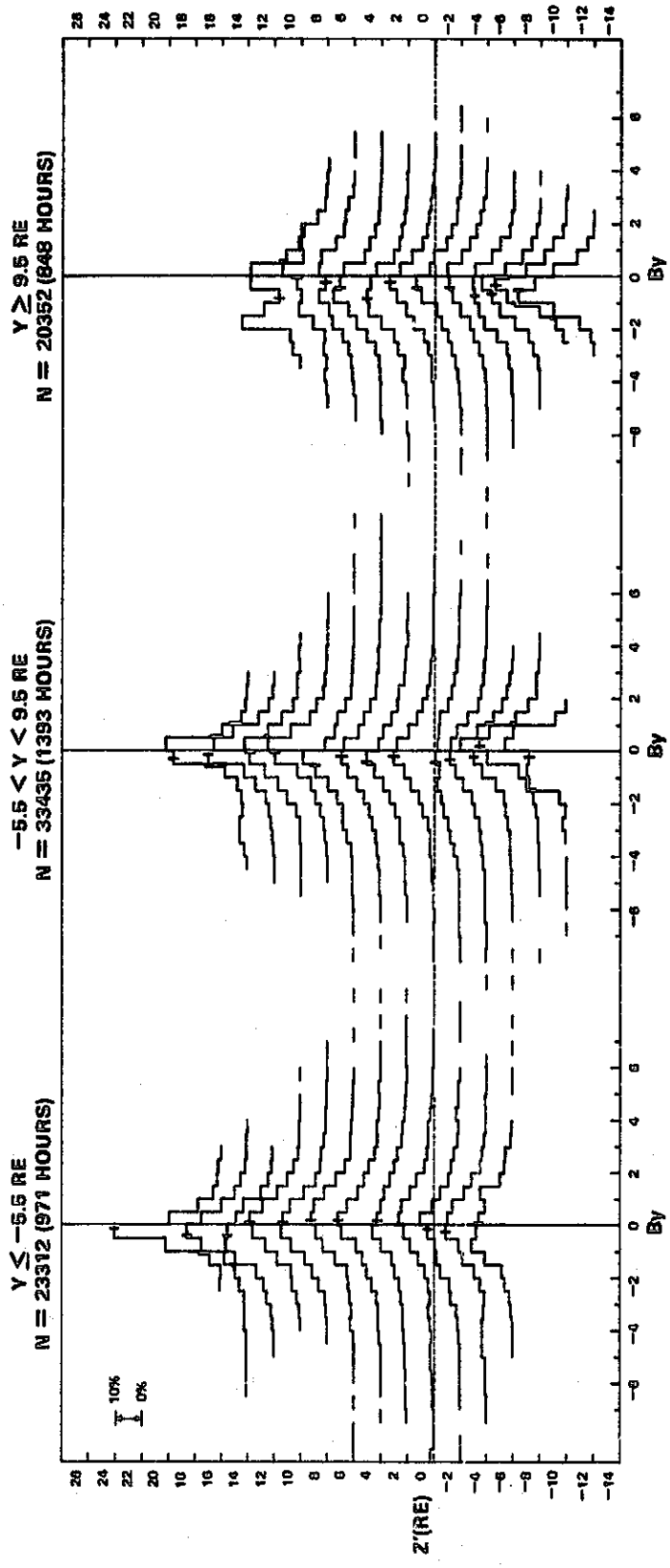

Figure 7

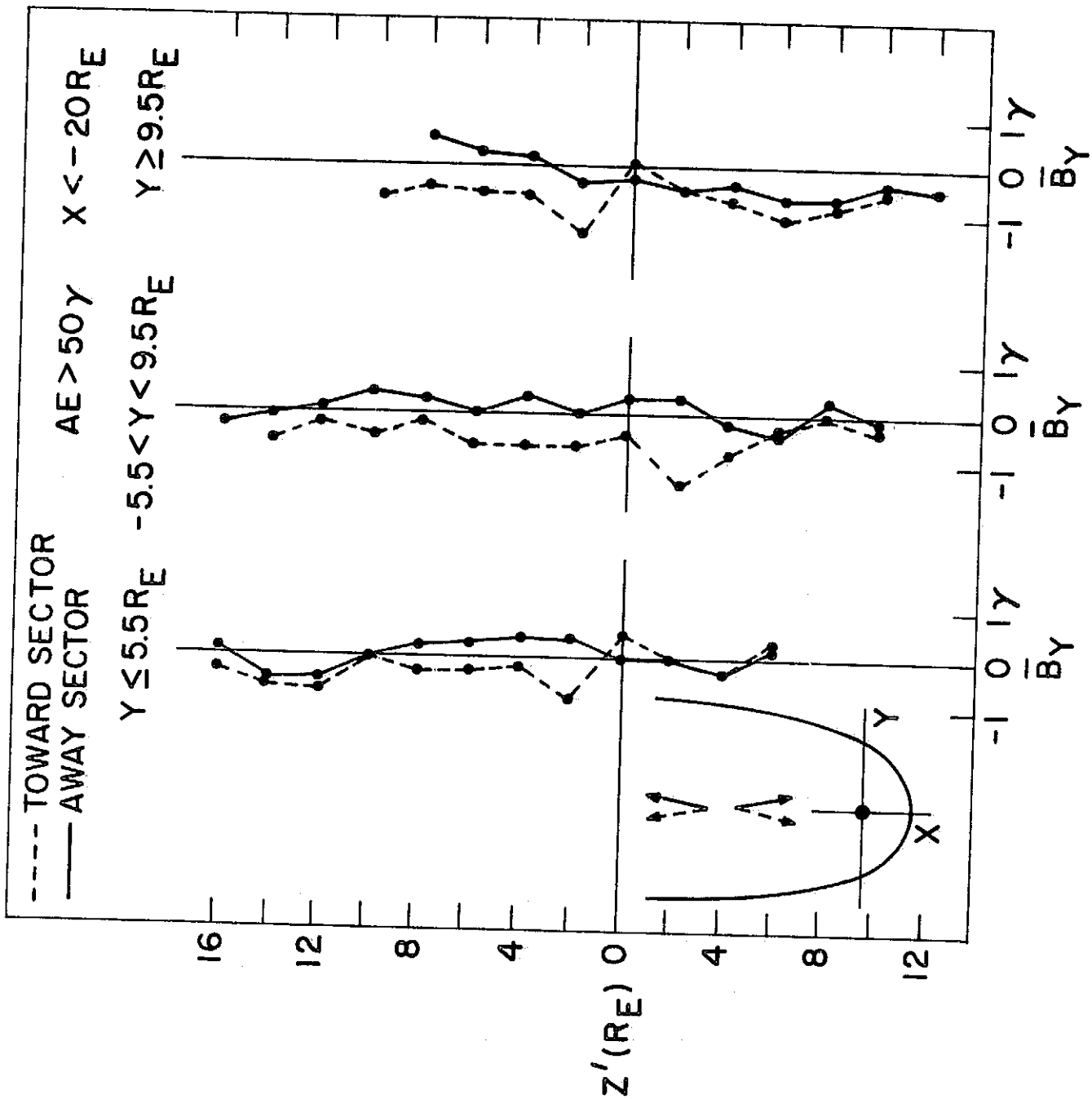
---- TOWARD SECTOR
—— AWAY SECTOR
AE > 50γ
X < -20R_E
Y ≥ 9.5R_E
-5.5 < Y < 9.5R_E
Y ≤ 5.5R_E
B̄_Y
Z'(R_E)
16
12
8
4
0
4
8
12
-1
0
1γ
Y
X

Figure 8

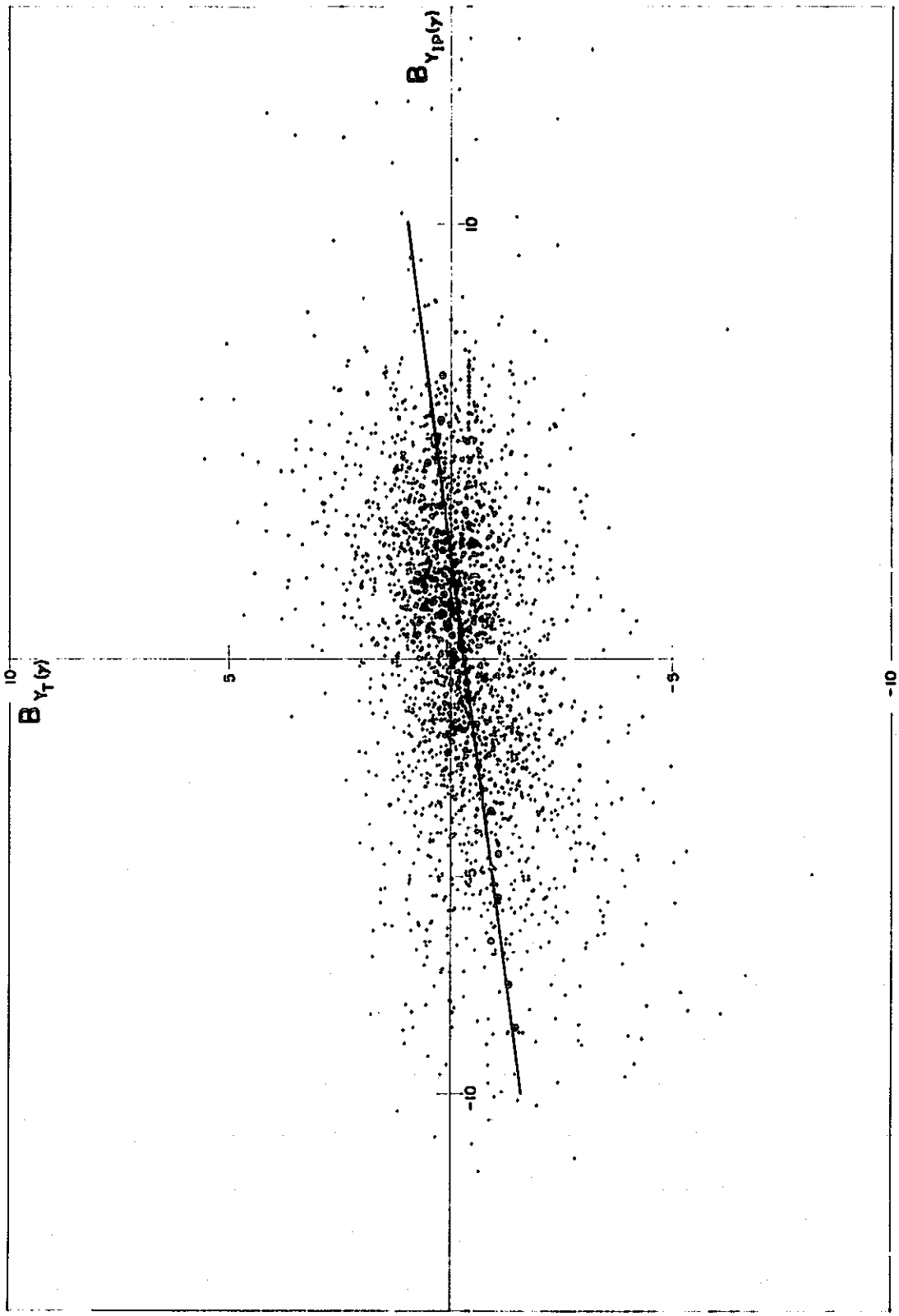

Figure 9

BIBLIOGRAPHIC DATA SHEET

1. Report No.	2. Government Accession No.	3. Recipient's Catalog No.
TM78116		

4. Title and Subtitle	5. Report Date
On The Configuration of the Geomagnetic Tail	March 1978
	6. Performing Organization Code: 695

7. Author(s)	8. Performing Organization Report No.
D. H. Fairfield	

9. Performing Organization Name and Address	10. Work Unit No.
Goddard Space Flight Center Planetary Magnetospheres Branch Greenbelt, Maryland 20771	11. Contract or Grant No.
	13. Type of Report and Period Covered: Technical Memorandum
12. Sponsoring Agency Name and Address	14. Sponsoring Agency Code

15. Supplementary Notes

16. Abstract

Over 3000 hours of IMP-6 magnetic field data obtained between 20 and 33 R_E in the geomagnetic tail have been used in a statistical study of the tail configuration. A distribution of 2.5 minute averages of B_Z as a function of position across the tail reveals that more flux crosses the equatorial plane near the dawn and dusk flanks ($\bar{B}_Z = 3.5\gamma$). The tail field projected in the solar magnetospheric equatorial plane deviates from the X axis due to flaring and solar wind abberation by an angle

$$\alpha = -0.9\ Y_{SM} - 1.7$$

where Y_{SM} is in earth radii and α is in degrees. After removing these effects the Y component of the tail field is found to depend on interplanetary sector structure. During an "away" sector the B_y component of the tail field is on average 0.5γ greater than that during a "toward" sector, a result that is true in both tail lobes and is independent of location across the tail. This effect means the average field reversal between northern and southern lobes of the tail is more often 178^o rather than 180^o that is generally supposed.

17. Key Words (Selected by Author(s))	18. Distribution Statement
Geomagnetic tail, equatorial plane	

19. Security Classif. (of this report)	20. Security Classif. (of this page)	21. No. of Pages	22. Price*
U	U	33	

*For sale by the National Technical Information Service, Springfield, Virginia 22151.